Influence of Cement Particle-Size Distribution on Early Age Autogenous Strains and Stresses in Cement-Based Materials

by
Dale P. Bentz
Building and Fire Research Laboratory
National Institute of Standards and Technology
Gaithersburg, MD 20899 USA

Ole Mejlhede Jensen
Aalborg University
DK-900 Aalborg, Denmark

Kurt Kielsgaard Hansen, John F. Olesen, and Henrik Stang
Technical University of Denmark
DK-2800 Lyngby, Denmark

Claus-Jochen Haecker
Wilhelm Dyckerhoff Institut
65203 Wiesbaden, Germany

Reprinted from the Journal of the American Ceramic Society, Vol. 84, No. 1, 129-135, 2001.

NIST
National Institute of Standards and Technology
Technology Administration, U.S. Department of Commerce

journal

J. Am. Ceram. Soc., 84 [1] 129–35 (2001)

Influence of Cement Particle-Size Distribution on Early Age Autogenous Strains and Stresses in Cement-Based Materials

Dale P. Bentz*

Building and Fire Research Laboratory, National Institute of Standards and Technology (NIST), Gaithersburg, MD 20899–8621, and Technical University of Denmark, DK-2800 Lyngby, Denmark

Ole Mejlhede Jensen

Aalborg University, DK-9000 Aalborg, Denmark

Kurt Kielsgaard Hansen, John F. Olesen, and Henrik Stang

Technical University of Denmark, DK-2800 Lyngby, Denmark

Claus-Jochen Haecker*

Wilhelm Dyckerhoff Institut, 65203 Wiesbaden, Germany

The influence of cement particle-size distribution on autogenous strains and stresses in cement pastes of identical water-to-cement ratios is examined for cement powders of four different finenesses. Experimental measurements include chemical shrinkage, to quantify degree of hydration; internal relative humidity development; autogenous deformation; and eigenstress development, using a novel embedded spherical stress sensor. Because the latter three measurements are conducted under sealed conditions, whereas chemical-shrinkage measurements are made under "saturated" conditions, the National Institute of Standards and Technology cement hydration and microstructure development model is used to separate the effects of differences in hydration rates (kinetics) from those caused by the different initial spatial arrangement of the cement particles. The initial arrangement of the cement particles controls the initial pore-size distribution of the cement paste, which, in turn, regulates the magnitude of the induced autogenous shrinkage stresses produced by the water/air menisci in the air-filled pores formed throughout the hydration process. The experimental results indicate that a small autogenous expansion (probably the result of ettringite formation), as opposed to a shrinkage, may be produced and early age cracking possibly avoided through the use of coarser cements.

I. Introduction

CEMENT-BASED materials are unique in that water, the same medium used for the hydration reactions and microstructural development, is also largely responsible for the degradation of the materials in service.[1] Although many degradation processes, such as the diffusion of chloride ions to induce corrosion of the steel reinforcement in reinforced concrete, occur over many years, others are induced by thermal and hydric loads very early in the life cycle of the structure. For example, one common problem, especially for newer, high-performance lower water-to-cement ratio (w/c) concretes, is early age cracking caused by self-desiccation and autogenous shrinkage[2,3] resulting from chemical shrinkage during the cement hydration process.[4,5]

As a cement paste hydrates under sealed conditions, chemical shrinkage occurs, because the hydration products occupy less space than the original reactants.[4,5] For a typical portland cement, this chemical shrinkage has a magnitude of ~0.06 g of water per gram of cement reacted.[4–6] In a sealed, unrestrained system, initially, the entire three-dimensional cement paste volume physically shrinks to match the chemical shrinkage, but once the cement has set (establishing a solid framework), this shrinkage is resisted and, instead, empty porosity is created within the capillary pore system of the cement paste microstructure. The water/air menisci created in these empty pores in turn induce an autogenous shrinkage (similar to a drying shrinkage[7]) of the cement paste that may result in cracking, under restrained conditions, if the tensile strain capacity of the material is exceeded. Cracking may occur globally, if the system is externally restrained, or locally, from the surfaces of the nonshrinking aggregate particles.[8,9] The magnitude of these autogenous stresses depends on the radius of the pores being emptied, as shown in Fig. 1 and Table I; hence, the initial pore-size distribution of the cement paste should have a strong influence on this process. Because the initial pore-size distribution is controlled, to a large extent, by the initial arrangement of the cement particles, cement fineness should be one material parameter that can be engineered to control/avoid autogenous shrinkage. Although computer modeling and some existing data in the literature have indicated that this should be the case,[10] the present paper presents experimental results for a cement clinker ground to four widely different finenesses which quantitatively demonstrate the validity of this hypothesis. Although Hua *et al.*[7] and Dela[8] have both demonstrated that stress relaxation and creep play a major role in the autogenous response of the hardening cement paste, we focus here only on the effects of cement particle-size distribution (PSD) on autogenous properties, with no attempt to quantify the significant influence of creep and stress relaxation on these measured experimental quantities.

H. M. Jennings—contributing editor

Manuscript No. 188803. Received January 18, 2000; approved July 17, 2000.
*Member, American Ceramic Society.

II. Experimental Procedure

The Bogue composition of the cement used in the present experimental study, as determined by quantitative microscopy,

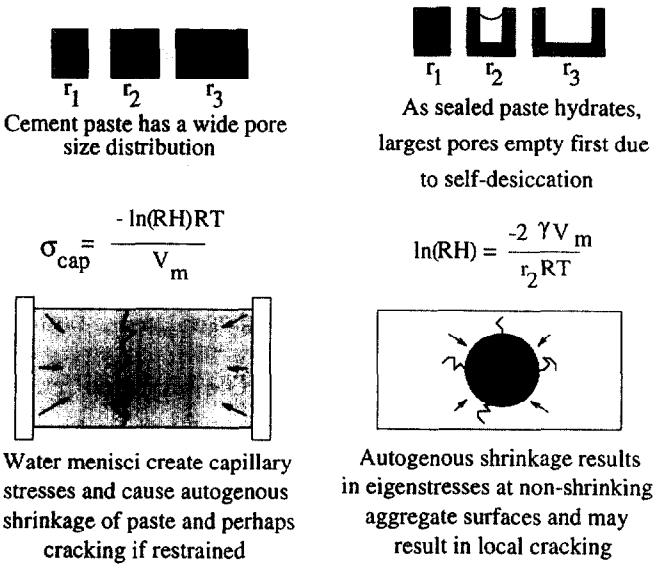

Fig. 1. Relation between pore-size distributions and autogenous strains and stresses in cement-based materials ("RH" is relative humidity; "γ" surface tension; "V_m" molar volume of water; "r_2" pore radius; "R" the universal gas constant; "T" temperature, in degrees Kelvin; and "σ_{cap}" capillary stress).

Table I. Capillary Stress versus RH and Pore Radius

Pore radius (μm)	RH (%)	σ_{cap} (MPa)
1.5	99.93	0.1
0.5	99.80	0.28
0.05	97.99	2.8
0.02	95.06	7.1

was 59% C_3S, 25.9% C_2S, 0.6% C_3A, and 14.2% C_4AF.[†] Rather than being interground with the cement, hemihydrate ($CSH_{1/2}$) was added at a mass percentage of 5%, just before mixing with water. This cement clinker was ground to four different finenesses, corresponding to Blaine finenesses[11] of 643, 387, 254, and 212 m^2/kg. The cumulative particle-size distributions for these four cement powders, as determined by laser diffraction techniques, are provided in Fig. 2. The corresponding average cement particle diameters, obtained by fitting a Rosin–Rammler distribution[12] to the shown distributions, are ~5, 15, 25, and 30 μm, respectively, proceeding from left to right in Fig. 2. All mixes were prepared with freshly boiled demineralized water.

For this study, w/c = 0.35 was chosen as low enough to minimize bleeding, while also high enough to avoid the necessity of using a water-reducing agent. For each mix, the cement powder was first dry-mixed with the hemihydrate addition. The appropriate mass of water was then added, and the paste was mixed for 5 min in a 5 L epicyclic standard mixer, with a brief pause after 2 min for scraping the sides of the bowl. The prepared paste was then cast in the holders for the various experimental measurements, as described in detail below. All specimens were subsequently cured at 30°C. This curing temperature was chosen to enhance the thermal stability of the oil and water baths and the environmental chamber used to hold the experimental equipment and specimens.

(1) Chemical Shrinkage

The chemical shrinkage of the cement pastes was measured following the general protocol developed by Geiker.[5] A small volume (typically 5.0 mm high) of cement paste of known mass was placed in a glass vial and covered with water. A rubber stopper containing a calibrated capillary tube was placed on top of the glass vial, establishing an initial height of water within the capillary tube. A small drop of paraffin oil was added on top of the water meniscus within the capillary tube, to minimize evaporative transfer. The vial was then secured in a constant-temperature water bath, and the chemical shrinkage was monitored by simply observing the drop in the water level in the capillary tube, with time. In general, measurements of chemical shrinkage were performed over the course of 28 d, and the results presented are the average for two specimens of similar heights. The maximum expanded uncertainty[13] in the calculated chemical shrinkage was estimated as 0.001 mL per gram of cement,[6] assuming a coverage factor of 2.[13]

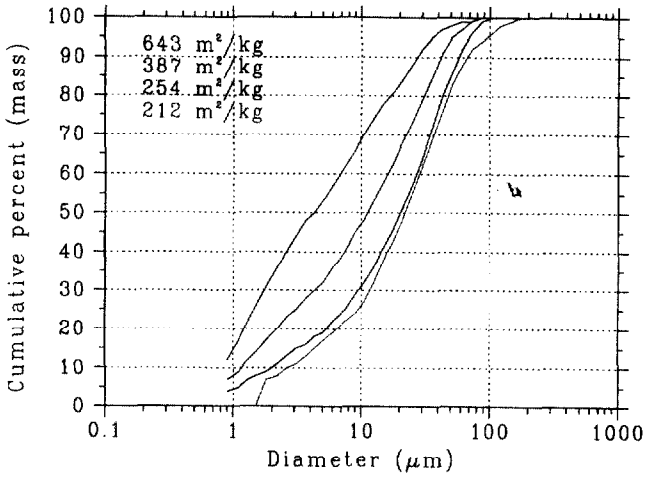

Fig. 2. Particle-size distributions for the cement powder ground to four different Blaine finenesses.

(2) Internal Relative Humidity

The internal relative humidity of the hydrating cement pastes was evaluated using a hygroscope (Hygroscope DT, Rotronic Instrument Corp., Huntington, NY)[‡] equipped with four measuring cells.[14] Before and after each experimental run, the equipment was calibrated using salt solutions with equilibrium relative humidity (RH) values between 75% and 100%. The equipment was contained in a thermostatically controlled box, with the temperature controlled to within ±0.1°C.

The fresh cement paste was simply placed in a sample holder that fit tightly into the sealed hygroscope cell. Typically, the volume of cement paste placed in the holder was a cylinder 42 mm in diameter and ~7 mm high. For most experiments, the freshly mixed paste was placed directly into the cell, and the change in RH was monitored immediately. However, for one experiment (with the 254 m^2/kg cement), to assess the contribution, if any, of bleeding to the RH readings, a companion sealed specimen was first rotated for 12 h (well beyond the setting time when any bleeding would cease) and then crushed and placed in a measuring cell. Bleeding was a concern for these experiments, because any expansion or lack of shrinkage observed for the coarser cements might possibly result from the readsorption of bleed water by the hydrating cement paste. The readings for this rotated/crushed specimen were virtually identical to those obtained on the virgin specimen, suggesting that, as expected, little or no bleeding occurred for these w/c = 0.35 specimens. The maximum standard deviation in RH between readings made on companion specimens

[†]Cement nomenclature: C is CaO, S is SiO_2, A is Al_2O_3, and F is Fe_2O_3 (therefore, C_3S is $3CaO{\cdot}SiO_2$).

[‡]Certain commercial equipment is identified by name in this paper to adequately specify the experimental procedure. In no case does such identification imply endorsement by the National Institute of Standards and Technology, nor does it imply that the products are necessarily the best available for the purpose.

was 0.48%, with average standard deviations for the four finenesses in the range 0.07%–0.23%.

(3) Autogenous Deformation

The autogenous deformation of the hydrating cement pastes was monitored using a custom-built dilatometer immersed in a constant-temperature (±0.1°C) oil bath.[15,16] The cement paste was cast into corrugated polyethylene tubes (~300 mm long, with an inner diameter of ~22 mm) that were sealed and placed in the dilatometer. There, linear displacement transducers were used to record the subsequent shrinkage/expansion of the tube during hydration of the enclosed cement paste. Typically, autogenous deformation was measured simultaneously on two nominally identical specimens, and the average result was reported.

The results reported in all plots are always relative to a deformation of zero at the time of set for the cement paste being evaluated. The setting time can be accurately determined by the abrupt change in slope in the original deformation-versus-time curves as the cement paste begins to offer a finite resistance to the autogenous deformation. After setting was achieved, the maximum standard deviation in relative deformation between readings made on companion specimens was 48.13 microstrains, with average standard deviations in the range 6.4–30 microstrains.

(4) Eigenstress Development

Eigenstresses were evaluated by embedding a special spherical stress sensor[8,17] in a cylindrical specimen (60 mm in diameter and ~60 mm high) of hydrating cement paste. The sensor consisted of two glass marble halves "glued" together (total diameter of ~16 mm) with an embedded manganin alloy wire. Manganin has the special property that its conductivity is dependent on the surrounding pressure and temperature of its immediate environment. Thus, by monitoring the conductivity of the manganin wire, the hydrostatic pressure surrounding the marble could be deduced. Calibration was performed in a pressurized oil bath, at constant temperature. For this study, temperature increases caused by hydration were minimized by placing the cylindrical mold containing the cement paste (and sensor) into a constant-temperature water bath. Still, all readings were corrected for the local temperature, which was measured using a thermocouple that was also embedded in the stress sensor. Based on readings made on companion specimens in a previous study,[8] the maximum standard deviation should be on the order of 0.5 MPa for stresses <10 MPa in magnitude.

III. Microstructural Modeling

To gain further insights into the influence of cement PSD on initial pore-size distribution and early age autogenous properties, the four experimental systems were also simulated using the National Institute of Standards and Technology (NIST) cement hydration and microstructure development model.[6,18] The measured PSDs (Fig. 2) and Bogue composition of the cements were used to create starting microstructures with w/c = 0.35. The starting microstructures were then hydrated under both saturated and sealed conditions,[6,18] to simulate the experimental conditions for the chemical shrinkage and autogenous measurements, respectively. By calibrating the chemical-shrinkage predictions of the model operated under saturated conditions to those observed experimentally, the degree of hydration versus time for hydration under sealed conditions could be inferred. This calculation made it possible to plot the observed autogenous measurements against degree of hydration (a material parameter), as well as against elapsed time, to separate differences in kinetics from those in microstructural features.

Two-dimensional slices from the initial three-dimensional microstructures for the four cement pastes are provided in Fig. 3. Clearly, the open "pores" between cement particles are much larger in the systems based on the coarser cements. To attempt to quantify this microstructural difference, a three-dimensional spherical adsorption/desorption program[19,20] was used to determine the pore volume accessible as a function of sphere diameter.

The algorithm is a rough estimation of adsorption/desorption in a porous media, because it assumes a spherical meniscus shape, whereas, in reality, a variety of three-dimensional ellipsoidal shapes are possible for the meniscus. For a sphere diameter of 1 μm (pixel), a conventional burning algorithm[21] is used to determine the accessible porosity. In this case, for all four w/c = 0.35 systems, nearly all the initial porosity is accessible. However, for a sphere diameter of 3 μm, large differences are observed between the four finenesses. The two cements with higher finenesses contain almost no porosity that is accessible for a diameter of 3 μm, whereas the two coarser cements contain significant pores (>50% of the total porosity) that are accessible to this sphere diameter. This finding suggests that, for a fixed amount of created empty porosity (resulting from self-desiccation), smaller pores would be emptied in the finer cement pastes than in the coarser ones. This difference should result in a more rapid decrease in autogenous relative humidity, an increased autogenous shrinkage, and, perhaps, an increase in the eigenstresses existing at an aggregate (or stress sensor) surface. This hypothesis is examined quantitatively in the following results.

IV. Results

(1) Internal Relative Humidity

The autogenous RH readings, with time, for the four cements studied are provided in Fig. 4. The spike observed at ~500 h for the 212 m^2/kg curve was caused by a temperature drop during a short power outage in the building, during which data continued to be collected, because the data logger runs on batteries. Each curve in Fig. 4 exhibits a similar behavior, with an initial increase (as the humidity sensor equilibrates with the cement paste) to a plateau region (98% to 98.5% RH), followed by a significant decrease, with time. The initial observed increase in RH does not reach 100% RH, because of the reduction in RH caused by the dissolved ions (Ca^{2+}, Na^+, etc.) present in the cement paste pore solution.[22] The coarser cements (254 and 212 m^2/kg) remain at their plateau level for a longer period of time and also subsequently decrease at a much slower rate than the finer cements (387 and 643 m^2/kg) for RH values between 98% and 96%, as hypothesized.

Of course, some of the differences in the curves shown in Fig. 4 result from the differing hydration kinetics of the four cements, because hydration rates are significantly influenced by cement PSD.[23,24] This finding could be examined preliminarily by plotting the internal relative humidity against the measured chemical shrinkage (directly proportional to the degree of hydration at early times[4–6]), the only problem being that the chemical-shrinkage specimens are basically saturated, whereas the internal-relative-humidity specimens experience sealed curing. One way around this minor discrepancy is to use the NIST cement hydration model, executed under both sealed and saturated curing conditions.[6,18]

Figure 5 shows a comparison of the model-predicted (saturated conditions) and the experimentally observed chemical-shrinkage results for the four different cement finenesses. As expected, the two finer cements hydrated at a significantly more rapid rate than did the coarser cements. For calibration of model hydration cycles to real time,[6] a simple linear calibration factor of 0.125 h/cycle was used for these specimens hydrated at 30°C. Thus, at a temperature of 30°C, the hydration behavior of these cements is better described by the linear, as opposed to the parabolic, kinetic model of Knudsen,[24] although the latter typically has been used for room-temperature hydration in past studies.[6,10,25] When this single calibration is used, good agreement is observed among all four experimental curves and their model counterparts (particularly for times between 10 and 200 h).

Next, the same calibration factor of 0.125 h/cycle was used for the simulated hydrations conducted under sealed conditions, to determine their degree of hydration versus time behavior. For each of the four systems, the achievable hydration values after 5 000 cycles (625 h) of model hydration, α_{5000}, under sealed and saturated

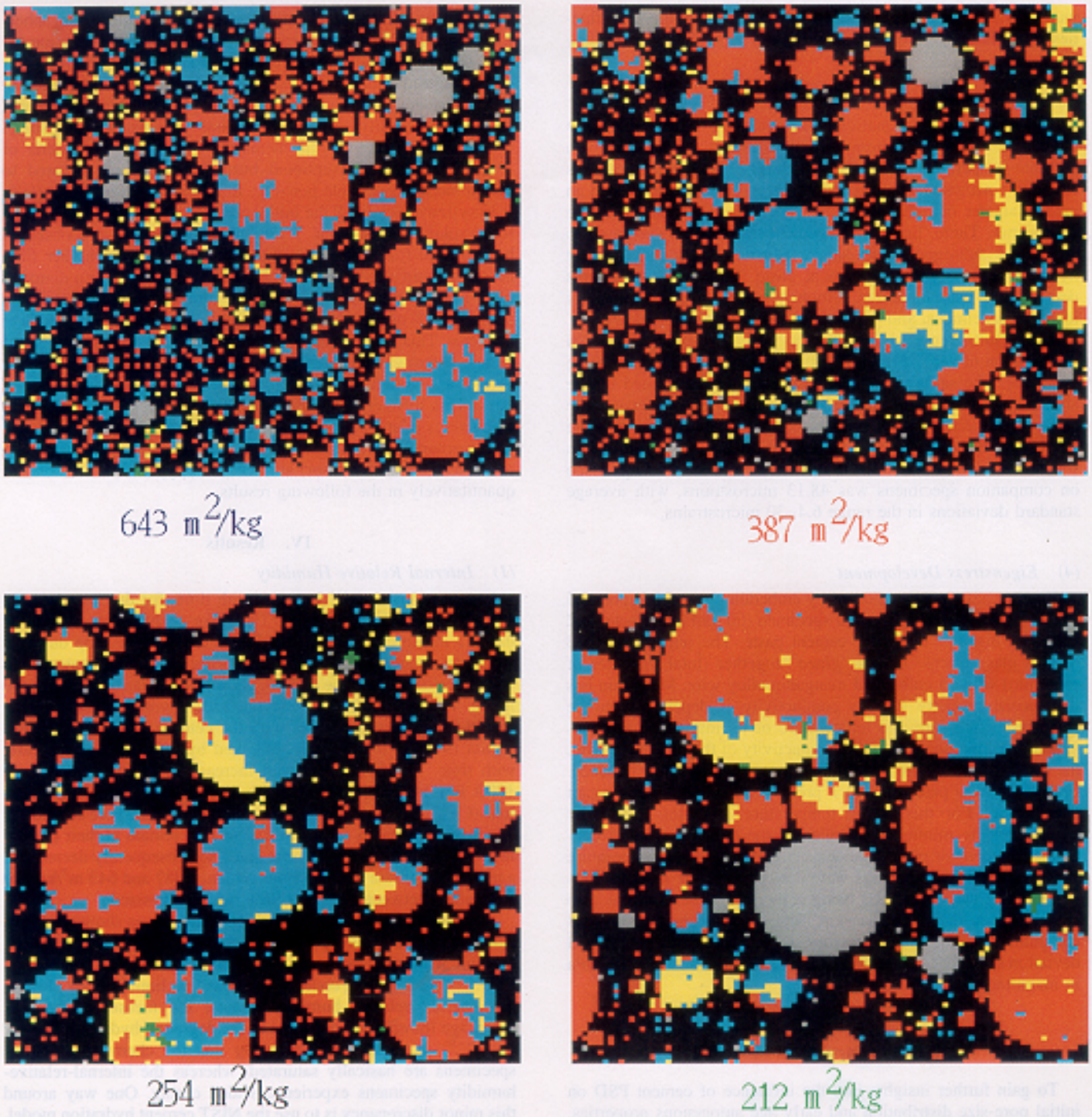

Fig. 3. Two-dimensional slices from three-dimensional model initial cement microstructures for the four different finenesses investigated in this study (color assignments: red—C_3S, blue—C_2S, green—C_3A, yellow—C_4AF, gray—hemihydrate, and black—capillary porosity; original images were 100 μm by 100 μm).

conditions are provided in Table II. As expected, the finer cements were able to achieve a higher degree of hydration and also exhibited a larger difference between sealed and saturated conditions. The sealed degree of hydration versus time was then used to plot the experimental relative humidity versus computed degree of hydration, as shown in Fig. 6. Interestingly, the plateau regions for all four finenesses now extend to the same degree of hydration, $\alpha = 0.4$. Beyond this, the curves basically diverge into two subsets, for the finer and coarser cements, respectively. The divergence is maximal at $\alpha \approx 0.47$, and then the two subsets of curves approach one another once again.

The curves in Fig. 6 can actually be interpreted as pore-size-distribution curves in the following manner. First, as shown in Fig. 1 and Table I, there is a direct relationship between RH and the size of the largest water-filled pore in the cement paste microstructure. Second, because the volume of empty porosity in a sealed system is directly proportional to the degree of hydration (after setting), the abscissa in Fig. 6 can be equivalently viewed as a measure of empty pore volume. Thus, Fig. 6 can be thought of as a plot of pore size versus (empty) pore volume. With this interpretation (and neglecting the effects of dissolved salts on RH), the sharp drop in RH with increasing hydration observed at $\alpha = 0.4$ for the two finer cements would indicate that these two microstructures contain significantly fewer "coarse" pores than do those based on the coarser cements, a result consistent with the microstructures shown in Fig. 3.

Although the differences in the RH-versus-α curves in Fig. 6 may seem rather subtle, the implications of those differences are

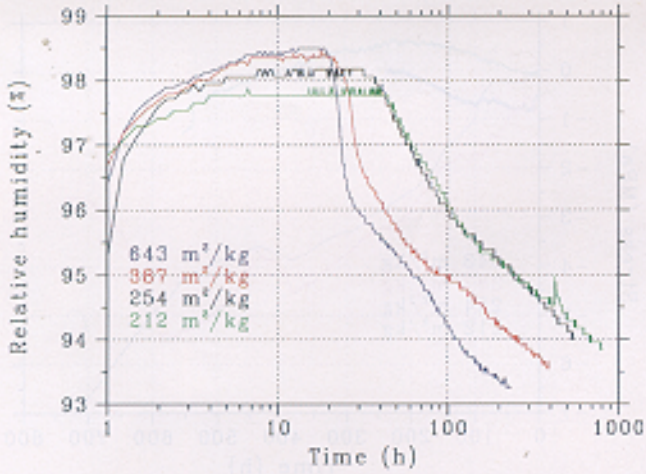

Fig. 4. Internal RH versus time, as a function of cement fineness.

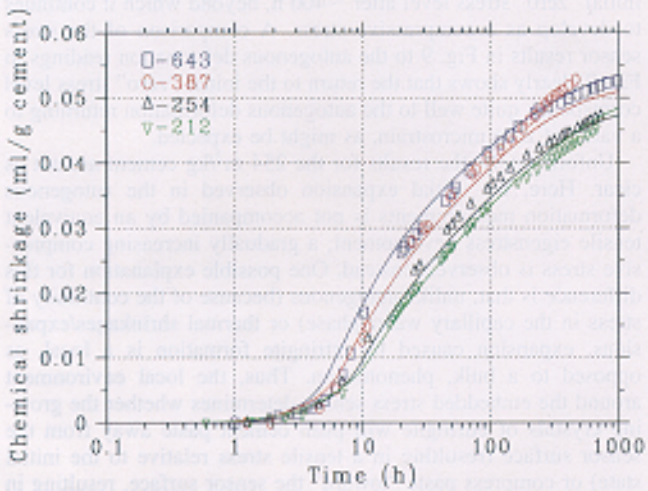

Fig. 5. Experimental (symbols) and model-predicted (solid lines) chemical shrinkage as a function of cement fineness. In all cases, the model was executed under saturated conditions, and hydration cycles were converted to time simply by multiplying by a factor of 0.125 h/cycle.

Table II. Computer Model Degrees of Hydration under Saturated and Sealed Conditions

Fineness (m^2/kg)	α_{5000} (saturated)	α_{5000} (sealed)
643	0.8561	0.7711
387	0.8079	0.7497
254	0.7520	0.7240
212	0.7549	0.7238

extremely significant, because the tensile strain capacity and elastic moduli of cement-based materials change drastically during the first several hundred hours of hydration.[7,8] Thus, delaying the development of "fine" water menisci and their associated stresses for just a few days should have a significant impact on minimizing autogenous shrinkage and cracking. At a fixed capillary stress (pore size), a microstructure that has hydrated more will have a higher elastic modulus and will have had a longer time for any stress relaxation and creep to manifest themselves. Thus, such a microstructure should exhibit less shrinkage. The autogenous deformation results presented next will, indeed, validate this conjecture.

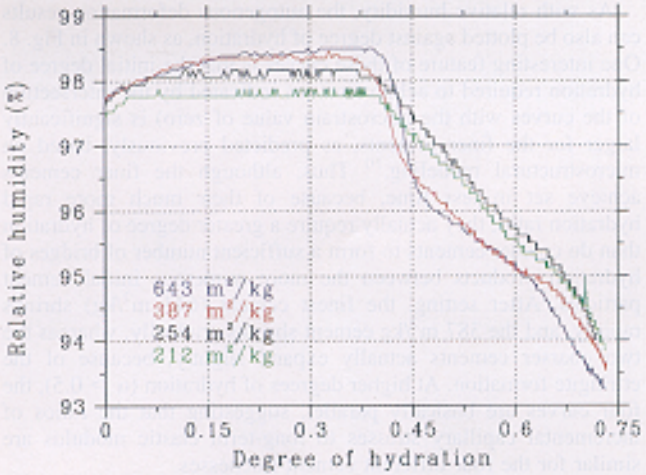

Fig. 6. Internal RH versus model-predicted degree of hydration, as a function of cement fineness.

(2) Autogenous Deformation

The measured autogenous deformation, versus time, of the four cements is shown in Fig. 7. For the two finest cements, a rapid development of shrinkage is observed, while the cement paste is relatively weak, followed by a more gradual development of shrinkage as the elastic modulus of the paste increases. For the coarser cements, after setting, a small initial expansion is produced, reaches a maximum, and then eventually is overwhelmed by the developing autogenous shrinkage. These general observations are consistent with comparable measurements of autogenous deformation versus cement fineness performed by Koenders[26] and by Tazawa and Miyazawa.[27] As with expansive type K cements,[28] the observed expansion most likely results from ettringite formation[29] (as opposed to readsorption of bleed water, which was eliminated as a possibility by the comparison of rotated and virgin-sealed RH specimens). Even though the cement is very low in C_3A content, substantial ettringite is formed from the reactions between the C_4AF phase and the hemihydrate, as measured by X-ray diffraction techniques for pastes with w/c = 0.5[30] and consistent with the observations of Fukuhara *et al.*[31] and of Brown.[32] Thus, in all four systems, there appears to be a competition between expansive ettringite formation and autogenous ("drying") shrinkage, with the latter clearly dominating for the finer cements.

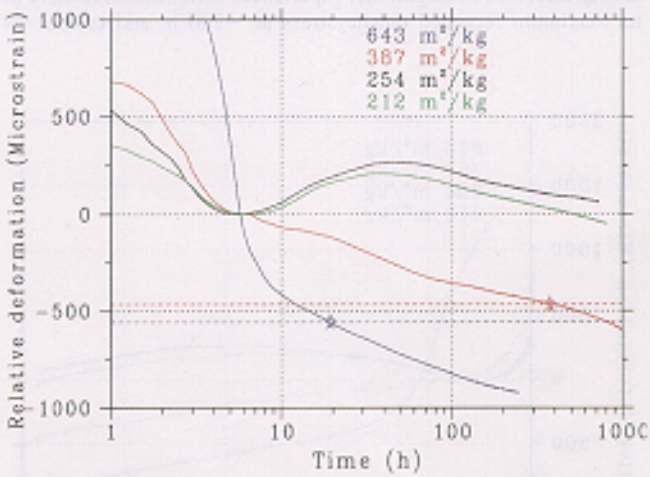

Fig. 7. Autogenous deformation versus time, as a function of cement fineness. Stars and colored broken lines indicate the microstrain levels corresponding to the hypothesized local cracking (stress reduction) around the embedded spherical stress sensor. Set time for each paste corresponds to the point where each curve first reaches a relative deformation value of zero.

As with relative humidity, the autogenous deformation results can also be plotted against degree of hydration, as shown in Fig. 8. One interesting feature of these curves is that the initial degree of hydration required to achieve set (as indicated by the intersection of the curves with the microstrain value of zero) is significantly larger for the finer cements, as predicted previously, based on microstructural modeling.[10] Thus, although the finer cements achieve set in less time, because of their much more rapid hydration rates, they actually require a greater degree of hydration than do coarser cements to form a sufficient number of bridges of hydration products between the more numerous initial cement particles. After setting, the finest cement (643 m^2/kg) shrinks rapidly, and the 387 m^2/kg cement shrinks gradually, whereas the two coarser cements actually expand slightly, because of the ettringite formation. At higher degrees of hydration ($\alpha > 0.5$), the four curves are basically parallel, suggesting that the ratios of incremental capillary stresses to long-term elastic modulus are similar for the four different cement finenesses.

(3) Eigenstress Development

Finally, we consider the results for the measurement of eigenstresses developing around the embedded spherical stress sensor, as shown in Fig. 9. In this figure, compressive stresses are shown as negative values and tensile stresses as positive ones, to agree with the sign convention used in the plots of autogenous deformation (i.e., an autogenous shrinkage corresponds to a compressive stress at the sensor surface). Once again, the four different cement finenesses exhibit quite distinct responses. The finest cement (643 m^2/kg) shows a small initial compressive stress, which decays steadily to a zero stress level. This steady decay probably results because the large initial autogenous shrinkage exceeds the tensile strain capacity of the young cement paste, causing local microcracking (and/or debonding) and stress relief at the sensor surface. A comparison of the eigenstress and autogenous deformation responses shows that this local microcracking is likely initiated at a strain level of about −560 microstrains. Interestingly, as shown by the broken colored lines and starred data points in Fig. 7, the 387 m^2/kg cement shows evidence for microcracking/damage initiating at about −460 microstrains. Thus, for both of these systems, the critical strain capacity appears to be on the order of −500 microstrains or 0.05%. Conversely, the critical stress levels are quite different for the two cement pastes, being ~0.8 and 4.5–5.5 MPa for the 643 and 387 m^2/kg cements, respectively.

The eigenstress behavior of the coarser cements is equally interesting. For the coarsest cement, from its initial state embedded in the fresh cement paste, the eigenstress sensor first registers a tensile stress (or a release from any initial compressive state) that slowly increases in magnitude, experiences compression relative to its maximum recorded tensile stress at ~200 h, and crosses its initial "zero" stress level after ~400 h, beyond which it continues to develop as a compressive stress. A comparison of the stress sensor results in Fig. 9 to the autogenous deformation readings in Fig. 7 clearly shows that the return to the initial "zero" stress level corresponds quite well to the autogenous deformation returning to a value of zero microstrain, as might be expected.

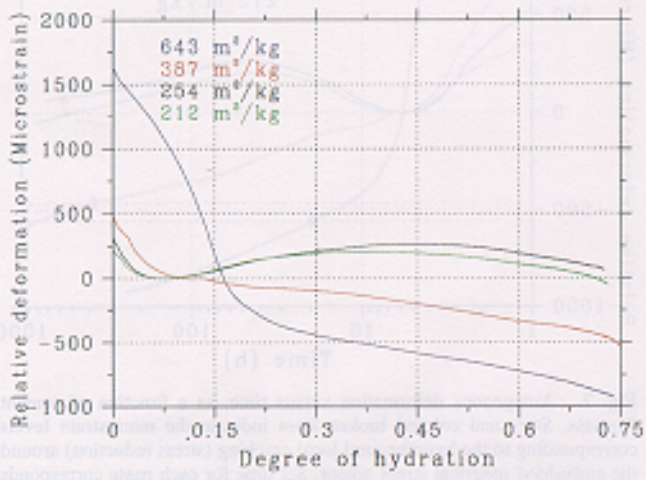

Fig. 8. Autogenous deformation versus model-predicted degree of hydration, as a function of cement fineness.

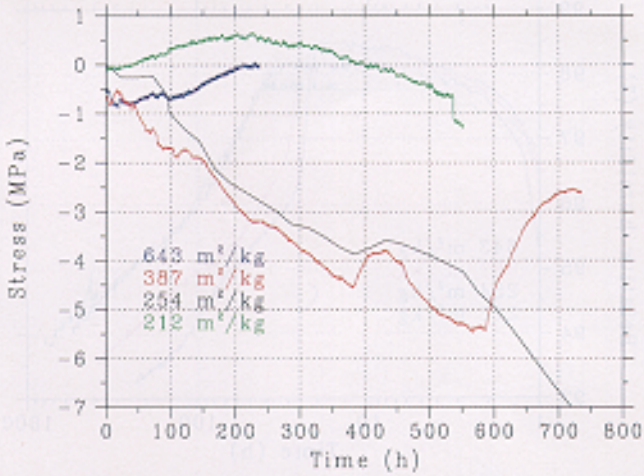

Fig. 9. Measured eigenstress versus time, as a function of cement fineness.

Unfortunately, the results for the 254 m^2/kg cement are not as clear. Here, the initial expansion observed in the autogenous deformation measurements is not accompanied by an equivalent tensile eigenstress development; a gradually increasing compressive stress is observed, instead. One possible explanation for this difference is that, unlike autogenous (because of the continuity of stress in the capillary water phase) or thermal shrinkages/expansions, expansion caused by ettringite formation is a local, as opposed to a bulk, phenomenon. Thus, the local environment around the embedded stress sensor determines whether the growing crystals of ettringite will push cement paste away from the sensor surface (resulting in a tensile stress relative to the initial state) or compress paste "toward" the sensor surface, resulting in an increase in local compressive stresses, as observed for the 254 m^2/kg cement. More important, from a practical viewpoint, despite the large compressive stress (7 MPa) ultimately developed at the stress sensor surface, there is little indication of microcracking, because the strain capacity of the paste is not exceeded in either compression or tension.

V. Discussion

The results presented above clearly indicate that cement PSD has a large role in determining the autogenous properties of hydrating cement paste. A further consideration in most high-performance concretes is the addition of mineral admixtures (pozzolans). For example, silica fume is composed of extremely fine (<1 μm) particles that will finely subdivide the initial pore structure of the paste. This subdivision, along with the further increase in self-desiccation caused by the pozzolanic reaction between silica fume and cement, results in large reductions in RH and large increases in autogenous shrinkage.[16] Conversely, fly ash particles are typically of a size similar to that of cement and would be expected to have a smaller detrimental influence on autogenous properties. This theory is consistent with the results of Houk *et al.*,[33] who studied a variety of concrete mixtures for the Dworshak Dam project and noted a "general increase in autogenous shrinkage with increase in fineness of the cementing materials." In their study,[33] "concretes containing fly ash had cementing materials of lowest overall fineness and exhibited lowest autogenous shrinkage."

The major problem in using coarser cements (and fly ashes) may be the lack of early age strength development. In general, minimizing cracking caused by autogenous (and thermal) shrinkage/expansion and maximizing early age strength appear to be

conflicting goals. If early age strength is not an issue, the ideal concrete might be one with a relatively low cement content,[33] a low w/c, and a relatively coarse initial pore-size distribution that densifies (to nearly zero capillary porosity) because of hydration. An alternate solution to the autogenous shrinkage and early age cracking problem is the use of saturated, lightweight aggregates to provide autogenous curing for these lower w/c concretes.[34,35] In these systems, the water initially saturating the pores in the lightweight aggregates is drawn into the hydrating cement paste by capillary forces, to provide the "extra" water needed to continue hydration and minimize capillary stresses and autogenous deformation. Thus, the reduction in RH will be controlled mainly by the size of the pores in the lightweight aggregates, which will be the first to empty because of self-desiccation.

VI. Conclusions

Careful experimental studies, using novel sensors, have demonstrated that cement particle-size distribution, through its influence on the initial pore-size distribution of fresh cement paste, has a significant effect on the early age autogenous properties of sealed specimens at identical w/c ratios. The larger pores present in the coarser cement paste reduce the rate of RH decay with increasing hydration, concurrently reducing the associated capillary stresses within the cement paste pore solution. In turn, both the autogenous shrinkage and the eigenstress (and associated microcracking) are reduced. Thus, engineering the PSD of the cement may be one method for reducing or eliminating early age cracking (both macro and micro) of high-performance concretes. Although coarse pores are relatively beneficial in minimizing early age cracking, they are detrimental to long-term strength, so that care must be taken in producing a concrete with optimum performance both in the short term and in future years. However, avoiding early age cracking is critical for the long-term durability of these high-performance materials.

The NIST microstructural model has been used successfully in conjunction with the present experiments, both to separate kinetics effects from true microstructure differences and to "quantify" the initial pore-size distribution of the cement pastes. Thus, this study demonstrates the synergistic effects of using a dual experimental/computer modeling approach to elucidate the complex relationships between microstructure and properties in cement-based materials.

Acknowledgments

The experimental measurements were performed during the summer of 1999, when D. P. Bentz was a visiting professor at the Department of Structural Engineering and Materials, Technical University of Denmark, funded by the Knud Hojgaard Foundation.

References

[1]*Materials Science of Concrete: Transport in Cement-Based Materials*. Edited by J. Marchand, J. J. Beaudoin, R. D. Hooton, and M. A. Thomas. American Ceramic Society, Westerville, OH, 2000.

[2]*Self-Desiccation and Its Importance in Concrete Technology*. Edited by B. Persson and G. Fagerlund. Lund Institute of Technology, Lund, Sweden, 1997.

[3]*Autogeneous Shrinkage of Concrete*. Edited by E. Tazawa. E & FN Spon, London, U.K., 1999.

[4]T. C. Powers, "Adsorption of Water by Portland Cement Paste during the Hardening Process," *Ind. Eng. Chem.*, **27**, 790–94 (1935).

[5]M. Geiker, "Studies of Portland Cement Hydration: Measurements of Chemical Shrinkage and a Systematic Evaluation of Hydration Curves by Means of the Dispersion Model"; Ph.D. Thesis. Technical University of Denmark, Lyngby, Denmark, 1983.

[6]D. P. Bentz, "Three-Dimensional Computer Simulation of Cement Hydration and Microstructure Development," *J. Am. Ceram. Soc.*, **80** [1] 3–21 (1997).

[7]C. Hua, P. Acker, and A. Ehrlacher, "Analyses and Models of the Autogenous Shrinkage of Hardening Cement Paste I. Modelling at Macroscopic Scale," *Cem. Concr. Res.*, **25** [7] 1457–68 (1995).

[8]B. F. Dela, "Eigenstresses in Hardening Concrete"; Ph.D. Thesis. Technical University of Denmark, Lyngby, Denmark, 1999.

[9]E. J. Garboczi, "Stress, Displacement, and Expansive Cracking Around a Single Spherical Aggregate under Different Expansive Conditions," *Cem. Concr. Res.*, **27** [4] 495–500 (1997).

[10]D. P. Bentz, E. J. Garboczi, C. J. Haecker, and O. M. Jensen, "Effects of Cement Particle Size Distribution on Performance Properties of Portland Cement-Based Materials," *Cem. Concr. Res.*, **29** [10] 1663–71 (1999).

[11]"Cement; Lime; Gypsum," ASTM Book of Standards, Vol. 04.01. American Society for Testing and Materials, West Conshohocken, PA, 1998.

[12]H. F. W. Taylor, *Cement Chemistry*. Thomas Telford, London, U.K., 1997.

[13]B. N. Taylor and C. E. Kuyatt, "Guidelines for Evaluating and Expressing the Uncertainty of NIST Measurement Results"; NIST Tech. Note No. 1297. U.S. Department of Commerce, Washington, DC, 1994.

[14]O. M. Jensen and P. F. Hansen, "Autogenous Relative Humidity Change in Silica Fume Modified Cement Paste," *Adv. Cem. Res.*, **7** [25] 33–38 (1995).

[15]O. M. Jensen and P. F. Hansen, "A Dilatometer for Measuring Autogenous Deformation in Hardening Portland Cement Paste," *Mater. Struct.*, **28**, 406–409 (1995).

[16]O. M. Jensen and P. F. Hansen, "Autogenous Deformation and Change of the Relative Humidity in Silica Fume Modified Cement Paste," *ACI Mater. J.*, **93** [6] 539–43 (1996).

[17]B. F. Dela and H. Stang, "Internal Eigenstresses in Concrete due to Autogenous Shrinkage"; see Ref. 2, pp. 46–55.

[18]D. P. Bentz, "Modelling Cement Microstructure: Pixels, Particles, and Property Prediction," *Mater. Struct.*, **32**, 187–95 (1999).

[19]D. P. Bentz, D. A. Quenard, V. Baroghel-Bouny, E. J. Garboczi, and H. M. Jennings, "Modelling Drying Shrinkage of Cement Paste and Mortar: Part I. Structural Models from Nanometers to Millimeters," *Mater. Struct.*, **28**, 450–58 (1995).

[20]D. P. Bentz, E. J. Garboczi, and D. A. Quenard, "Modelling Drying Shrinkage in Porous Materials Using Image Reconstruction: Application to Porous Vycor Glass," *Modell. Simul. Mater. Sci. Eng.*, **6**, 211–36 (1998).

[21]D. P. Bentz and E. J. Garboczi, "Percolation of Phases in a Three-Dimensional Cement Paste Microstructural Model," *Cem. Concr. Res.*, **21** [2] 325–44 (1991).

[22]G. Hedenblad, "Moisture Permeability of Mature Concrete, Cement Mortar, and Cement Paste"; Ph.D. Thesis. Lund University of Technology, Lund, Sweden, 1993.

[23]J. M. Pommersheim, "Effect of Particle Size Distribution on Hydration Kinetics"; pp. 301–306 in *Materials Research Society Symposium Proceedings*, Vol. 85. Materials Research Society, Pittsburgh, PA, 1987.

[24]T. Knudsen, "The Dispersion Model for Hydration of Portland Cement: I. General Concepts," *Cem. Concr. Res.*, **14**, 622–30 (1984).

[25]D. P. Bentz and C. J. Haecker, "An Argument for Using Coarse Cements in High Performance Concretes," *Cem. Concr. Res.*, **29** [4] 615–18 (1999).

[26]E. A. B. Koenders, "Simulation of Volume Changes in Hardening Cement-Based Materials"; Ph.D. Thesis. Delft University of Technology, Delft, The Netherlands, 1997.

[27]E. Tazawa and S. Miyazawa, "Influence of Cement and Admixture on Autogenous Shrinkage of Cement Paste," *Cem. Concr. Res.*, **25** [2] 281–87 (1995).

[28]C. Lobo and M. D. Cohen, "Hydration of Type K Expansive Cement Paste and the Effects of Silica Fume: I. Expansion and Solid Phase Analysis," *Cem. Concr. Res.*, **22**, 961–69 (1992).

[29]O. M. Jensen, "Influence of Cement Type upon Autogenous Deformation and Change of the Relative Humidity"; Tech. Note, Chemistry Department, University of Aberdeen, Aberdeen, Scotland, August 1995.

[30]C. J. Haecker, unpublished results, 1998.

[31]M. Fukuhara, S. Goto, K. Asaga, M. Daimon, and R. Kondo, "Mechanisms and Kinetics of C_4AF Hydration with Gypsum," *Cem. Concr. Res.*, **11**, 407–14 (1981).

[32]P. W. Brown, "Kinetics of Tricalcium Aluminate and Tetracalcium Aluminoferrite Hydration in the Presence of Calcium Sulfate," *J. Am. Ceram. Soc.*, **76** [12] 2971–76 (1993).

[33]I. E. Houk Jr., O. E. Borge, and D. L. Houghton, "Studies of Autogenous Volume Change in Concrete for Dworshak Dam," *ACI J.*, **66** [45] 560–68 (1969).

[34]S. Weber and H. W. Reinhardt, "Manipulating the Water Content and Microstructure of High Performance Concrete Using Autogenous Curing"; pp. 567–77 in *Modern Concrete Materials: Binders, Additions, and Admixtures*. Edited by R. K. Dhir and T. D. Dyer. Thomas Telford, London, U.K., 1999.

[35]D. P. Bentz and K. A. Snyder, "Protected Paste Volume in Concrete: Extension to Internal Curing Using Saturated Lightweight Fine Aggregate," *Cem. Concr. Res.*, **29** [11] 1863–67 (1999). □